Large magnetocaloric effect in Dy_2NiSi_3

Jean J Mboukam, Baidyanath Sahu, André M Strydom

Highly Correlated Matter Research Group, Physics Department, University of Johannesburg, PO Box 524, Auckland Park 2006, South Africa

E-mail: jules.mboukam@gmail.com

Abstract. The intermetallic ternary compound Dy_2NiSi_3 crystallizes in the AlB_2 type of hexagonal structure with the space group P6/mmm. The magnetic properties were studied by measuring magnetization as a function of temperature, and magnetic field and heat capacity ($C_p(T)$) in magnetic fields up to 7 T. Temperature dependent magnetization and heat capacity results revealed that Dy_2NiSi_3 shows an antiferromagnetic (AFM) ordering with Néel temperature at 5.9 K. Below the magnetic phase transition, $C_p(T)$ data is described by a spin wave spectrum with an energy gap of $\Delta = E/k_B = 1.96(4)$ K. The magnetocaloric effect (MCE) of the compound has been evaluated from heat capacity measurements and maximum values of magnetic entropy change and adiabatic temperature change are found to be 20.3 J/kg.K and 11.3 K respectively for a field change up to 7 T.

1. Introduction

Rare-earth based intermetallic compounds are attractive due to their novel magnetic properties such as: magnetocrystalline anisotropy and metamagnetism, spin-glass, heavy fermion behaviour, magnetoresistance effect, and magnetocaloric effect (MCE). In particular, there is great interest on the topic of MCE for magnetic refrigeration. MCE has advantages for environmental-friendly, energy-generation features [1, 2], which can replace the traditional vapour compressor technology and carbon-based fuels in the future. MCE is defined as the isothermal entropy change ($-\Delta S_M$) or adiabatic temperature change ($\Delta T_{\rm ad}$) of magnetic materials upon application of a magnetic field. MCE is a magneto-thermodynamic phenomenon which is observed in practically all magnetic materials when the material is cooled down sufficiently under magnetic field. RE_2NiSi_3 (where RE stands for rare-earth elements) compounds crystallize in the hexagonal AlB_2-type structure. One of the interesting features in these compounds is the co-existence of long-range AFM ordering and magnetically frustrated spin-glass behaviours [3, 4, 5, 6]. Beside these behaviours, several members in this system exhibit large MCE over a wide temperature range due to spin fluctuation [6, 7]. It is also reported that the MCE of RE_2NiSi_3 compounds may become enhanced in a defect structure [6].

In this work, single-phase sample material of polycrystalline Dy_2NiSi_3 was prepared. The magnetic properties, specific heat and MCE derived from calorimetric measurements of the compound have been systematically studied.

2. Experimental Details

Polycrystalline Dy_2NiSi_3 was prepared under high purity argon gas by a standard arc-furnace melting technique using stoichiometric amounts of high purity elements of Dy (99.99%), Ni

(99.999%) and Si (99.99%). The sample was turned over and remelted several times in order to ensure homogeneity. The sample was then wrapped in a tantalum foil and encapsulated in an evacuated quartz tube under 6.3 $\times 10^{-6}$ mbar pressure. The ingot was then heat treated at 1123 K for 7 days in a Carbolite box furnace followed by room-temperature water quenching. Powder x-ray diffraction measurements were carried out at room temperature using a Rigaku diffractometer employing the CuKα_1 radiation (λ = 1.540598 Å). Structural and phase purity analyses were confirmed by refinement of the powder x-ray diffraction patterns using the FullProf programme [8]. Temperature dependent dc-magnetic susceptibility was measured using a commercial Dynacool Physical Property Measurement System from Quantum Design (San Diego) with a vibrating sample magnetometer from 1.8 K to 50 K in applied magnetic field of 0.1 T. The heat capacity measurements were carried out in the temperature range between 1.8 K to 20 K in different fields of 0, 1, 3, 5 and 7 T using the same Dynacool PPMS system.

3. Results and discussion

The XRD-pattern of Dy_2NiSi_3 measured at room temperature is shown in Fig. 1 along with the Rietveld least-square refinement. All the diffraction peaks can be indexed in the hexagonal AlB_2-type structure with space group $P6/mmm$ (No. 191). In this refinement, the Dy (blue balls) atoms occupy the crystallographic 1a position while Ni and Si (red and white balls, respectivelly) atoms share the 2d site (see inset of Fig. 1). This was as also reported in [9]. The obtained refinement was clear with no impurity phase detectable on the patterns as shown in Fig. 1. The obtained lattice parameters and unit cell volume are: a = 3.9607(2) Å, c = 4.0258(3) Å and V = 54.69(2) Å^3, respectively. These values are in agreement with the previous study [10].

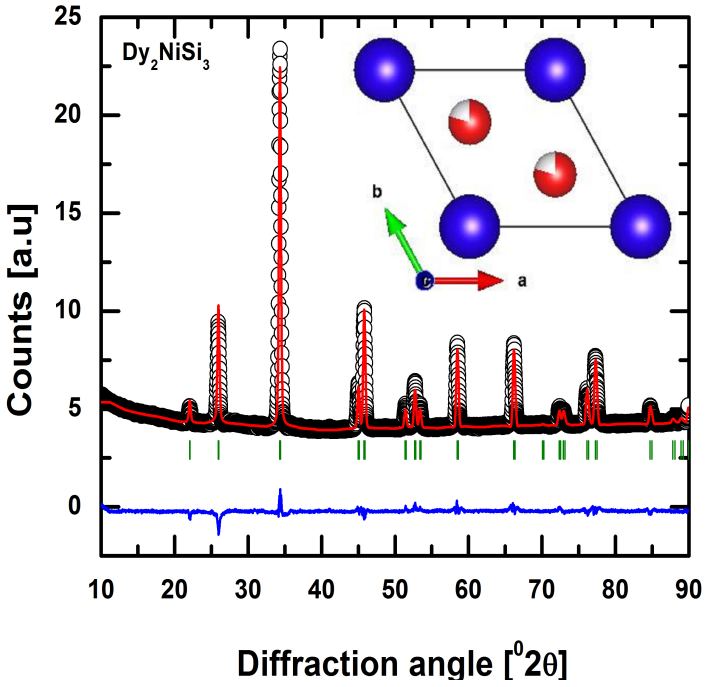

Figure 1: (Color online) The X-ray diffraction pattern (black symbols) of Dy_2NiSi_3 collected at room temperature and its Rietveld refinement (red curve). The bottom blue curve represents the difference between the experimental and calculated patterns. The vertical (green) ticks represent the calculated Bragg's reflection positions. The inset shows the crystal structure of Dy_2NiSi_3 with Dy, Ni and Si atoms at their crystallographic positions.

Fig. 2a shows the temperature dependence of dc-magnetic susceptibility, $\chi(T)$ (left axis) and inverse dc-magnetic susceptibility, $\chi^{-1}(T)$ (right axis) of Dy_2NiSi_3 compound measured from 1.8 K - 50 K under an applied magnetic field of 0.1 T. $\chi(T)$ data of Dy_2NiSi_3 displays a phase transition at around $T_N = 5.9$ K as indicating by the arrow, probably of AFM origin. Above the magnetic transition, $\chi^{-1}(T)$ data are linear in temperature and follow the Curie-Weiss relation:

$$\chi^{-1} = \frac{3k_B(T - \theta_P)}{N_A \mu_{eff}^2}, \tag{1}$$

where k_B and N_A are respectively the Boltzmann and Avogadro constant, θ_P is the paramagnetic Weiss temperature and μ_{eff} is the effective magnetic moment. The black line on $\chi^{-1}(T)$ data represents the least-square fit using Eq.1. This yielded $\theta_P = -0.81(1)$ K and $\mu_{eff} = 10.46(2)$ μ_B. The obtained μ_{eff} is very close to that expected for the free trivalent Dy ion (10.63 μ_B). The negative θ_P hints to an AFM exchange interactions. In Fig. 2b, the magnetization, $M(\mu_0 H)$ (blue symbols) measured at 2 K for field change up to 7 T shows a linear behaviour up to the critical field $\mu_0 H_{meta} = 0.8$ T where a weak field-induced metamagnetic transition occurs, and a tendency of saturation at high field. These can be connected to a complex (metamagnetic interactions) and or multiple type of interactions such as ferromagnetic (FM) and AFM interactions in the compound. Such type of analysis has also been performed on other reported compounds [9, 11, 12, 13]. The critical field ($\mu_0 H_{met}$) was estimated from the derivative of $dM(\mu_0 H)/dH$ and was taken at its maximum (see black symbols) as shown by the arrow. In order to study the nature of the magnetic phase transition, Arrott plots for the mean field model were made as shown in Fig. 2c. According to Banerjee's criterion, the negative slopes (see inset Fig. 2c) observed in low magnetic field and below T_N indicate the first order nature of the magnetic transition, whereas the positive slopes correspond to a second order magnetic phase transition [14].

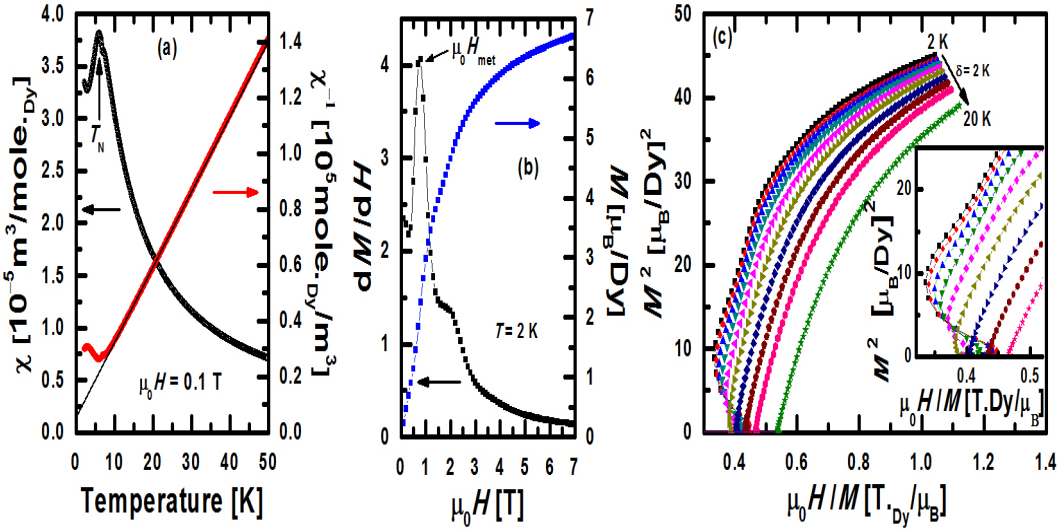

Figure 2: (a) Temperature dependence of the magnetic susceptibility of Dy_2NiSi_3 measured from 1.8 K - 50 K under an applied magnetic field of 0.1 T (left axis). Plot on the right hand axis shows the inverse magnetic susceptibility with the Curie-Weiss fit (black line) as described in the text. (b) Magnetization data measured at 2 K (blue symbols) along with dM/dH (black symbols). (c) Arrott plots for the mean field theory measured in the temperature range 2 K - 20 K in step of 2 K. The inset shows an expanded view of M^2 versus $\mu_0 H/M$.

The heat capacity of Dy_2NiSi_3 as a function of temperature measured in different magnetic fields of 0, 1 3, 5, and 7 T are shown in Fig. 3a and Fig. 3b, respectively. As seen in Fig. 3a,

$C_{\rm p}(T)$ data at 0 T show a peak that is plausibly associated with an AFM phase transition at $T_N = 5.9$ K. The obtained transition temperature is in agreement with T_N obtained from $\chi(T)$ measurements (see section **??**). This peak indicates the presence of long-range magnetic order, similar to that observed for the other reported compounds [6, 15, 16, 17]. The ordered region ($T<T_N$) of $C_p(T)$ is described by the AFM spin wave spectrum, which was fitted (see line in Fig. 3a) using the expression [18]:

$$C_{\rm p}(T) = \gamma_{AFM} T + BT^3 exp\left(-\frac{\Delta}{T}\right), \tag{2}$$

which takes into account the magnon contribution described by an energy gap ($\Delta = E/k_B$, where E is the energy). B is a constant. The fit yielded the values of the Sommerfeld coefficient γ_{AFM} = 1.39(5) J/mole.$_{\rm Dy}$.K^2, $B = 0.055(5)$ J/mole.$_{\rm Dy}$.K^4 and $\Delta = 1.96(4)$ K. As seen in Fig. 3b, an increasing of magnetic field gradually suppresses T_N, which shifts toward low-temperatures as expected for AFM materials.

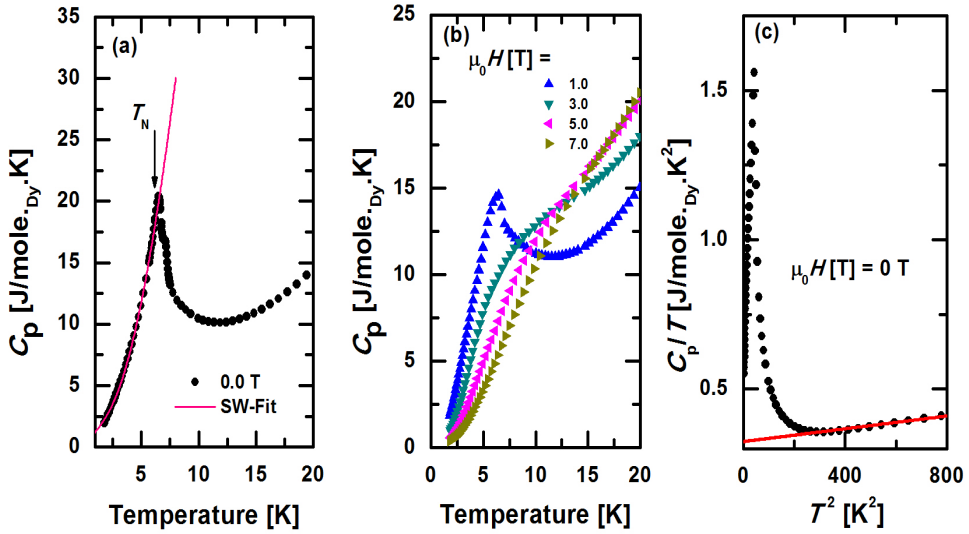

Figure 3: Temperature variation of $C_{\rm p}(T)$, of Dy_2NiSi_3 measured (a) in 0 T and (b) in different applied magnetic field of 1, 3, 5 and 7 T, where the arrow indicated the position of T_N. (c) Shows the linear dependence of $C_{\rm p}(T)/T$ versus T^2 in the paramagnetic region, above $\sim$ 20 K.

Fig. 3c shows $C_p(T)/T$ versus T^2 with a linear dependence in the paramagnetic region ($T>T_N$), indicating the electronic contribution to the heat capacity. The red curve is the least-square fit using the expression:

$$C_{\rm p}(T)/T = \gamma_P + \beta T^2. \tag{3}$$

The obtained values from the fit are: $\gamma_P = 0.32(3)$ J/mole.$_{\rm Dy}$.K^2, $\beta = 1.07 \times 10^{-4}(5)$ J/mole.$_{\rm Dy}$.K^2 and $\theta_{\rm D} = 224.73$ K derived from $\theta_D = (12\pi^4 nR/5\beta)^{1/3}$, where n and R in this latter equation represent the number of atoms ($n = 6$) per formula unit and the gas constant, respectively. The greater value of the Sommerfeld coefficient γ_{AFM} in the AFM region which is about 4 times greater than γ_P may be due to the electron-electron interactions when the 4f spins engage in AFM order below T_N.

In order to investigate the MCE properties from the calorimetric measurements of Dy_2NiSi_3, $C_{\rm p}(T)$ was measured at different magnetic fields up to 7 T. MCE refers to a change of the

magnetic entropy ($-\Delta S$) induced by an applied field that can be evaluated from $C_{\rm p}(T)$ using the Maxwell thermodynamic relationship [1]:

$$\Delta S(T, \mu_0 H) = \int_0^T \left(\frac{C_{\rm p}(T')_{\mu_0 H} - C_{\rm p}(T')_0}{T'} \right) d(T'), \tag{4}$$

where $C_{\rm p}(T)_{\mu_0 H}$ and $C_{\rm p}(T)_0$ represent the heat capacity measured at applied and zero magnetic field respectively.

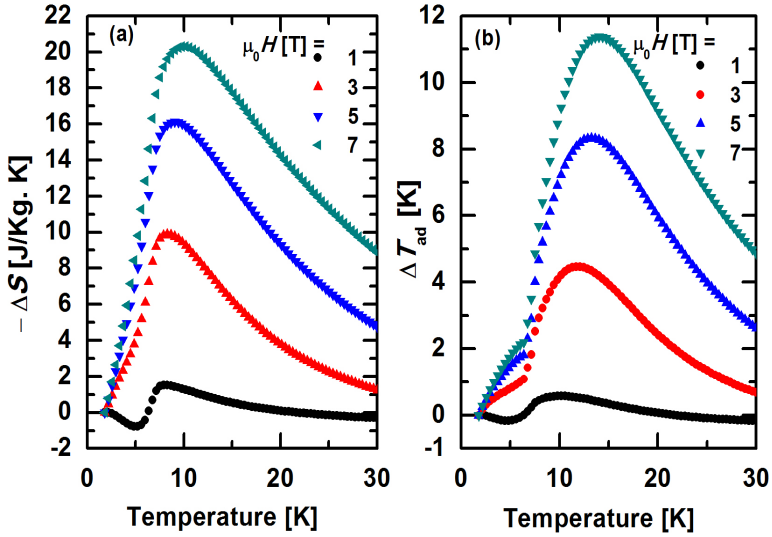

Figure 4: (a) Temperature dependencies of the entropy change $-\Delta S(T)$ calculated in fields of 0, 1, 3, 5 and 7 T, together with their respective adiabatic temperature change $\Delta T_{\rm ad}$ in (b).

Fig. 4a displays $-\Delta S(T)$ of Dy_2NiSi_3 as a function of temperature for different applied magnetic field changes up to 7 T. This was calculated using Eq. 4. It is clearly seen that relatively small negative $-\Delta S(T)$ values are observed below T_N for low magnetic field change. This is in agreement with field-induced metamagnetic behaviour [19, 20]. The obtained maximum values of $-\Delta S(T)$ evaluated using Eq.4 are 1.8, 10.1, 16.02 and 20.3 J/kg.K at $T = 5.9$ K, for fields change of 1, 3, 5 and 7 T, respectively. $-\Delta S(T)$ obtained at 7 T for this compound is higher than those of various promising magnetic refrigerant materials [13, 21, 22, 23, 24] and very close to that obtained from the isothermal magnetization studies in a defect structure of the same compound [9].

Another important factor for good refrigerant materials is the adiabatic temperature change ($\Delta T_{ad}(T)$) defined as:

$$\Delta T_{\rm ad} = [T(S, \mu_0 H) - T(S, 0)]_S \,, \tag{5}$$

where $T(S, \mu_0 H)$ and $T(S, 0)$ denote the temperature at applied and zero magnetic field for the particular $-\Delta S^{max}(T)$, respectively. The value of $\Delta T_{\rm ad}(T)$ was evaluated using $-\Delta S(T, \mu_0 H)$ and zero field heat capacity data. Fig. 4b displays the adiabatic temperature change $\Delta T_{ad}(T)$ for Dy_2NiSi_3. The obtained maximum value of $\Delta T_{\rm ad}(T)$ is 11.3 K for Dy_2NiSi_3 under a field change of 7 T. Even for a low field change of 5 T, $\Delta T_{\rm ad}(T)$ is 8.3 K, which is beneficial for application purpose. This value is comparable to the one of his counterpart metamagnetic $Ho_2Ni_{0.93}Si_{2.93}$ material obtained at 7 T [11] and other good magnetic materials [25, 26]. The nature of $\Delta T_{\rm ad}(T)$

is almost similar to $-\Delta S(T)$. Large positive values of $-\Delta S(T)$ and $\Delta T_{\rm ad}(T)$ are also observed above a field change of 1 T. This is due to the field induced first order metamagnetic transition as it was also reported in other metamagnetic compounds [9, 11, 12, 26].

4. Summary

A synthesized polycrystalline compound of Dy_2NiSi_3 was found to crystallize with the hexagonal AlB_2 type structure with the space group P6/mmm. The compound exhibits a first order nature of the magnetic phase transition as confirmed in an Arrott plots construction. The ordered region of $C_p(T)$ is characterized by a spin wave spectrum with an energy gap, $\Delta = 1.96(4)$ K. $-\Delta S(T)$ and $\Delta T_{\rm ad}$ measured from the heat capacity measurements reach the values of 20.3 J/kg.K and 11.3 K, respectively for a field change of 7 T. These obtained values are higher or similar to the same isostructural systems, RE_2CuSi_3 with RE = Pr and Gd [25] and in defect crystal structure $Tm_2Ni_{0.93}Si_{2.93}$ [26]. The obtained MCE values can classify Dy_2NiSi_3 amongst promising candidates for magnetic refrigerants.

Acknowledgments

AMS thanks the FRC/URC of UJ and the National Research Foundation (NRF) for financial support. Baidyanath Sahu thanks the UJ-GES postdoctoral fellowship for the support.

References

[1] Tishin AM, Spichkin YI, *The magnetocaloric effect and its application.* Eds. Coey JMD, Tilley DR, Vij DR (Institute of Physics Publishing, Bristol, 2003)
[2] Gschneidner Jr KA, Pecharsky VK, Tsokol AO, 2005 Rep. *Prog. Phys.* **68** 1479
[3] Li DX, Nimori S, Yamamura T, Shiokawa Y, 2008 *J. Appl. Phys.* **103** 07B715
[4] Pan ZY, Cao CD, Bai XJ, Song RB, Zheng JB, Duan LB, 2013 *Chinese Phys. B.* **22** 056102
[5] Hwang JS, Lin KJ, Tien C, 1996 *Solid State Commun.* **169** 100
[6] Pakhira S, Mazumdar C, Ranganathan R, Giri S, 2016 *Phys. Rev.* B. **94** 104414
[7] Zhitomirsky ME, 2003 *Phys. Rev.* B. **67** 104421
[8] Roisnel T, Rodrquez-Carvajal J, 1999 *Mater. Sci. Forum* 2001 **378** 118
[9] Pakhira S, Mazumdar C, Choudhury D, Ranganathan R, Giri, 2018 *Phys. Chem. Chem. Phys.* B. **20** 13580
[10] Chen X, Zhuang Y, 2016 *Phase Transit.* **90** 742
[11] Pakhira S, Mazumdar C, Ranganathan R, Avdeev M, 2017 *Sci. Rep.* **7** 7367
[12] Mboukam JJ, Tchoula Tchokonte MT, Bashir AK, Sondezi BM, Sahu BN, Strydom AM, Kaczorowski D, 2020 *J. Alloys Compd.* **814** 152228
[13] Samanta T, Das I, Banerjee S, 2007 *Appl. Phys. Lett.* **91** 152506
[14] Banerjee SK, 1964 *Phys. Lett.* **12** 16
[15] Tien C, Fen CH, Wur CS, Lu JJ, 2000 *Phys. Rev.* B. **61** 12151
[16] Jona YM, Sakai O, Higashinaka R, Fukazawa, H, Maeno Y, Dasgupta P, Ghosh D, 2003 *Phys. Rev.* B. **68** 174413
[17] Anand VK, Adroja DT, Hillier AD, Taylor J, Andre G, 2011 *Phys. Rev.* B. **84** 064440
[18] Tari A *The specific heat of matter at low temperatures.* (Imperial College Press, 2003)
[19] Alho BP, Nbrega EP, De Sousa VS, Carvalho AM, De Oliveira NA, Von Ranke PJ, 2011 *J. Appl. Phys.* **109** 083942.
[20] Wang YX, Zhang H, Wu ML, Tao K, Li YW, Yan T, Long KW, Long T, Pang Z, Long Y, 2016 *Chin. Phys. B.* **25** 127104
[21] Hu WJ, Du J, Li B, Zhang Q, Zhang ZG T, Das I, Banerjee S, 2008 *Appl. Phys. Lett.* **92** 192505
[22] Gupta S, Rawat R, Suresh KG, 2014 *Appl. Phys. Lett.* **105** 012403
[23] Mboukam JJ, Sondezi BM, Tchoula Tchokonte MB, Bashir AKH, Strydom AM, Britz D, Kaczorowski D, 2018 *Physica B.* **536** 505
[24] Tchoula Tchokonte MB, Mboukam JJ, Bashir AKH, Sondezi BM, Ramesh Kumar K, Strydom AM, Kaczorowski D, 2018 *Physica B.* **753** 41
[25] Wang F, Yuan FY, Wang JZ, Feng TF, Hu GQ, 2014 *J. Alloys Compd.* **592** 63
[26] Pakhira S, Mazumdar C, Ranganathan R, 2017 *J. Phys. Condens. Matter* **29** 505801